ACS OMEGA

http://pubs.acs.org/journal/acsodf

Article

Multinetwork Elastomer Using Covalent Bond, Hydrogen Bond, and Clay Plane Bond

Keisuke Chino*

Cite This: *ACS Omega* 2021, 6, 31168−31176

Read Online

ACCESS | Metrics & More | Article Recommendations

ABSTRACT: A high-performance elastomer was obtained by a multinetworking system of a covalent bond, hydrogen bond, and clay plane bond. By taking advantage of the characteristics of each cross-linking, the thermoplastic elastomer shows excellent compression set resistance, good flowability, and high tensile properties. The hydrogen bond gives flowability due to the bond cleavage under heating. The covalent bond contributes to the low compression set by prevention of polymer chain flow. Moreover, the clay plane bond affects the tensile properties by de-localization of the entire cross-link and increase of hysteresis energy between the clay plane surface and other cross-linking points. Furthermore, the self-healing properties and high heat resistance and recyclability were also observed.

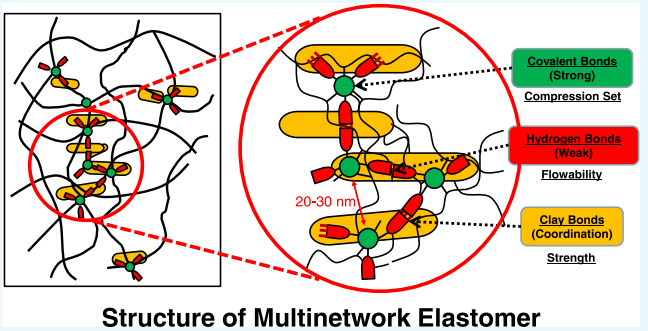

1. INTRODUCTION

Cross-linking is one of the most important factors for rubber properties. Since Charles Goodyear invented sulfur vulcanization in 1839, the rubber industry has been developed so far. Since the interaction between rubber chains consisting of hydrocarbons is very weak, the rubber cannot show good mechanical properties without cross-linking. Therefore, the rubber goods are cross-linked by covalent bonds such as sulfur or peroxide cross-links. However, since the covalent bond, which has a high bond energy, cannot be cleaved by heating, the rubber cannot be remolded. Hence, more than 50% of the worn-out tires are burned as a thermal energy source without material recycling. Reusage of the waste vulcanized rubber as a raw material is an urgent issue for environmental conservation. On the other hand, the thermoplastic elastomer is cross-linked by physical interaction between the polymer chains instead of a covalent bond. Since the physical cross-linking can be easily cleaved by heating, the thermoplastic elastomer can be remolded. However, since the bonding energy of the physical interaction is low, the mechanical properties, especially compression set, are poor.

A double-network system using different kinds of cross-links had been applied to the rubber. For example, double networks consisting of sulfur and peroxide cross-links had been reported to increase the strength of the rubber.[1−6] Moreover, in the field of gel science, double networks using strong and weak cross-links have been reported to increase the strength, because the weak cross-link is destroyed sacrificially to dissipate energy, prior to breaking of the strong cross-linkage.[7] Furthermore, Haraguchi reported that a high-strength gel can be obtained by clay plane cross-linking[8] because clay plane cross-linking points interact with the polar groups of polymers and dissipate energy under external stresses. Consequently, since the stress concentration to the polymer chain is prevented, the strength of the gel increases.

Before we have developed thermoreversible cross-linking rubber, which is recyclable, reformable, and has similar mechanical properties to vulcanized rubber at room temperature, by using hydrogen bonds.[9−12] However, the compression set of the elastomer was high (poor) owing to the cleavage of the hydrogen bonds under heating. Compression set is one of the most important properties for rubber goods. If the compression set is high, the rubber goods cannot be used due to deformation.

In this article, we tried to develop a high-performance elastomer by using a multinetwork system comprising a covalent bond, hydrogen bond, and clay plane bond. The covalent bond is expected to affect the compression set due to the stable cross-linkage. However, introduction of a covalent bond may deteriorate the tensile properties. Therefore, we try to further introduce clay plane cross-linking, which is expected to increase the hysteresis energy to improve the tensile properties.[13] Moreover, the hydrogen bond gives flowability due to the

Received: August 25, 2021
Accepted: October 28, 2021
Published: November 11, 2021

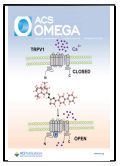

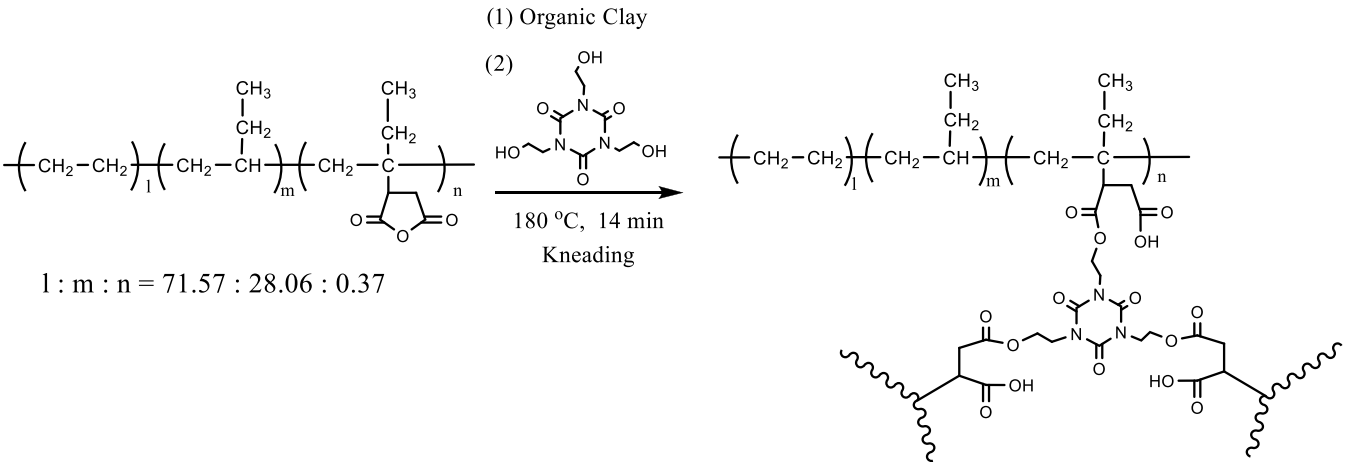

Figure 1. Synthesis of a multinetwork elastomer.

bond cleavage under heating. Research on a multi-cross-linking system using a hydrogen bond, covalent bond, and clay bond has never been reported so far.

If the total energy of the covalent bond, hydrogen bond, and clay plane bond can be the same as that of normal rubber cross-link, the multinetwork elastomer (MNE) may show the same characteristics as the normal rubber at room temperature, and develop fluidity by cleavage of the hydrogen bond under heating.

2. RESULTS AND DISCUSSION

2.1. Synthesis and Properties. As a method of introducing hydrogen bonding and covalent bonding moiety to the elastomer, addition reactions of maleic anhydride moiety followed by reaction of active hydrogen compounds, in the solid phase, have been used due to the following reasons: (1) Since the addition reaction of active hydrogen compounds with the cyclic acid anhydride moiety has been known to proceed effectively, the solid mixing reaction of a maleated elastomer with active hydrogen compounds was expected to proceed effectively. (2) The addition reaction of cyclic acid anhydride and active hydrogen compounds was also expected to generate covalent cross-linking and strong hydrogen bonding moieties such as carboxylic acid, ester, and amide. (3) Since the addition reaction of maleic anhydride to elastomer has been widely used in the industry as the easiest method to introduce polar groups,[14,15] maleated elastomers are easily available on the industrial market.

Maleated ethylene-butene elastomer was selected as a base elastomer, because of its low hardness, low T_g, and sufficient mechanical properties. The low hardness of the elastomer should be derived from low crystallinity. The introduction reaction of active hydrogen compounds to the maleated ethylene-butene elastomer was performed at 180 °C by using an internal mixer (Figure 1).

The reaction of the hydroxyl and amine groups of various active hydrogen compounds with the acid anhydride ring was confirmed by IR and solid-state NMR analyses. The introduction of active hydrogen compounds was identified by the disappearance of the absorption peaks at 1790 cm^{-1} due to acid anhydride, as well as the existence of the peaks due to ester or imide.

The properties of the obtained elastomer are shown in Table 1.

Table 1. Formulations and Properties of Test Samples

run	1	2	3	4	5
maleated ethylene-butene rubber	100	100	100	100	100
organic clay			5	5	5
3-amino-1,2,4-triazol (ATA)	1.26				
tris(2-hydoxyethyl)isocyanurate (THI)		1.31	1.31		
polyether polyol				3.83	
sulfamide					0.72
antioxidant[a]	0.1	0.1	0.1	0.1	0.1
hardness	57	39	66	62	66
tensile strength (MPa)	4.82	1.34	8.22	6.92	5.45
elongation at break (%)	628	108	181	446	545
compression set (%)	80	16	17	39	96

[a]3-(3,5-Ditert-butyl-4-hydroxyphenyl)propanoic acid.

As a hydrogen bond cross-linking, 3-amino 1,2,4-triazole was reacted with the maleated ethylene-butene elastomer.[1−4] In this case (Table 1 run 1), although the tensile strength and the elongation at break are sufficient, the compression set is high (poor). Cleavage of the hydrogen bonds under heating may result in the high compression set. Next, as a cross-linker that can generate covalent and hydrogen bonds simultaneously, tris(2-hydroxyethyl)isocyanurate (THI) was selected. THI can generate 3 covalent cross-linking points and the isocyanurate ring can form hydrogen bonds with carboxylic acid and ester, which is generated by the reaction of the maleic anhydride moiety and the hydroxyl group. Although the tensile strength and the elongation at break are low, the compression set is low (good). The low compression set might be caused by the stable covalent cross-linking under heating (Table 1 run 2). Meanwhile, the low tensile strength and the low elongation at break should be caused by the lack of hysteresis energy. Since stress may concentrate on specific points due to the lack of hysteresis energy, the elastomer structure may be broken quickly. In order to improve the tensile properties by prevention of the stress concentration, clay was added (Table 1 run 3, Figure 1). Clay is expected to increase the hysteresis energy by interaction with the hydrogen bond cross-link. It has been reported that addition of clay can increase the strength of the gel.[8] First, bentonite was selected as a clay. However, untreated bentonite cannot be dispersed sufficiently in the elastomer. Therefore, organic clay was used in order to improve the dispersion. Addition of the organic clay before introduction of hydrogen bond and covalent

https://doi.org/10.1021/acsomega.1c04633
ACS Omega 2021, 6, 31168−31176

bond gave better properties than addition of organic clay after the introduction of hydrogen and covalent bond. Addition of the organic clay before the cross-linking may give high dispersion because the cross-linking network in an elastomer is surmised to prevent the sufficient dispersion of clay. When the organic clay was added before the formation of cross-linking, the tensile strength and elongation at break were improved without deterioration of the compression set. The dispersion of organic clay is discussed in "Section 2.4".

Next, in order to find the best cross-linking agent that can generate the hydrogen bond and covalent bond, various chemicals were examined. As representative examples, polyetherpolyol and sulfamide are shown in run 4 and 5, respectively. Since polyether polyol has 4 same-length linkers, improvement of the compression set was expected by uniformity of the length of cross-linking.[16] Since sulfamide has a planar structure, increase of mechanical properties was also expected by formation of two-dimensional hydrogen bonds.[17] Although both compounds gave good tensile properties, the compression sets were not sufficient. The reason for the remarkable properties of THI as a cross-linking agent may be the interaction of hydrogen bonds of the isocyanurate ring, ester, and carboxylic acid, in addition to the stable covalent bonds.

2.2. Effect of Varying Amounts of Organic Clay. Successively, amounts of the organic clay and THI were investigated (Table 2).

Table 2. Effect of Amounts of THI and Organic Clay

run	1	2	3	4	5	6
maleated ethylene-butene rubber	100	100	100	100	100	100
organic clay	0	1	2.5	2.5	2.5	5
tris(2-hydoxyethyl) isosianurate (THI)	1.31	1.31	0.983	1.31	1.64	1.31
antioxidant[a]	0.1	0.1	0.1	0.1	0.1	0.1
hardness	39	57.5	58	61.5	62.5	65.5
100% modulus	1.35	2.08	2.45	3.14	4.51	5.66
300% modulus		3.77	4.97	6.86		
tensile strength (MPa)	1.34	3.88	4.69	6.78	7.78	8.22
elongation at break (%)	108	291	296	308	233	181
compression set (%)	16	38	39	2	5	17

[a]3-(3,5-Ditert-butyl-4-hydroxyphenyl)propanoic acid.

Since the addition of organic clay could increase the hysteresis energy and improve the tensile properties, the amount of organic clay was investigated.

Addition of 0, 1, 2.5, and 5 phr (parts per hundred rubber, Table 2 runs 1, 2, 4, 6) of the organic clay were investigated (Figure 2). In conclusion, elongation at break, which indicates dispersion, was highest around 2 phr of the clay. The tensile strength was saturated to 7−8 MPa more than 2.5 phr of the clay.

2.3. Effect of Varying Amounts of THI. Next, in 2.5 phr addition of clay, 0.75 (Table 2 run 3), 1 (Table 2 run 4), and 1.25 (Table 2 run 5) equiv of the hydroxyl group of THI against the maleic anhydride moiety were investigated (Figures 3 and 4). Since 0.75 equiv of THI is less than the molar stoichiometry of maleic anhydride moiety, the cross-linking density should decrease and the elongation at break may be improved.

Moreover, since 1.25 (Table 2 run 5) equiv is more than the molar stoichiometry of the maleic anhydride moiety, the branch of THI increase and the cross-linking density should decrease, which may also improve the elongation at break. However, 1 equiv (Table 2 run 4) of THI gave the best elongation at break and the best compression set. It indicates that 1 equiv gave the most efficient cross-linking structure.

The properties of the obtained elastomer (Table 2 run 4) are shown in Table 3.

The glass transition temperature (T_g) of the obtained elastomer, which is observed by a dynamic viscoelasticity analyzer, was almost the same as that of the starting maleated ethylene-butene elastomer (T_g: −40.4 °C). It indicates that cross-linkages do not disturb the micro-Brownian motion of the main chain segment. The obtained elastomer has similar good properties at low temperature (*ex.* low brittle temperature) to the starting elastomer.

Moreover, the 5% weight loss temperature was very high (405 °C), which is higher than that of the general thermoplastic elastomer. The obtained elastomer had thermoplasticity and can be recycled at least 10 times without deterioration of the properties. It was confirmed that the tensile strength after 10 times reforming was maintained at 94% (6.37 MPa) of the initial strength. Moreover, the self-healing temperature, which can adhere itself by heating, was confirmed at 140 °C. The 1 mm thickness sheet having a 5 mm notch was heated by elevating the temperature by 20 °C from 60 °C and was kept under each temperature for 10 min. Adhesion of the notch was confirmed at 140 °C, which can be derived from the recombination of hydrogen bonds (adhesion strength 4.61 MPa, retention rate

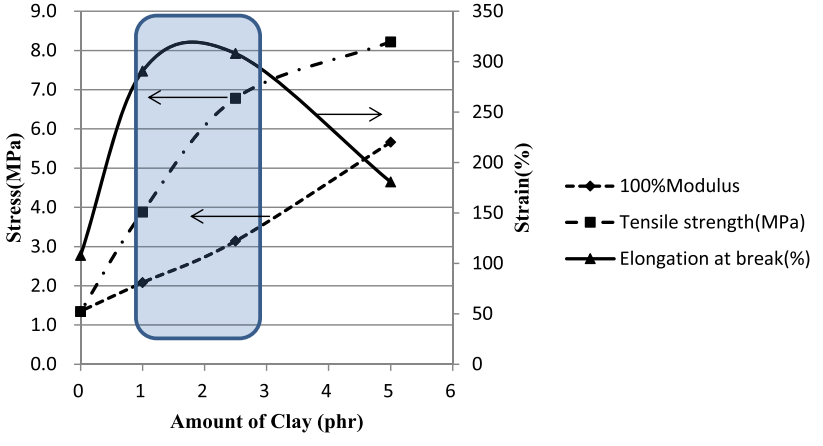

Figure 2. Correlation between amount of clay and stress or strain in the presence of 1 equiv of THI.

https://doi.org/10.1021/acsomega.1c04633
ACS Omega 2021, 6, 31168−31176

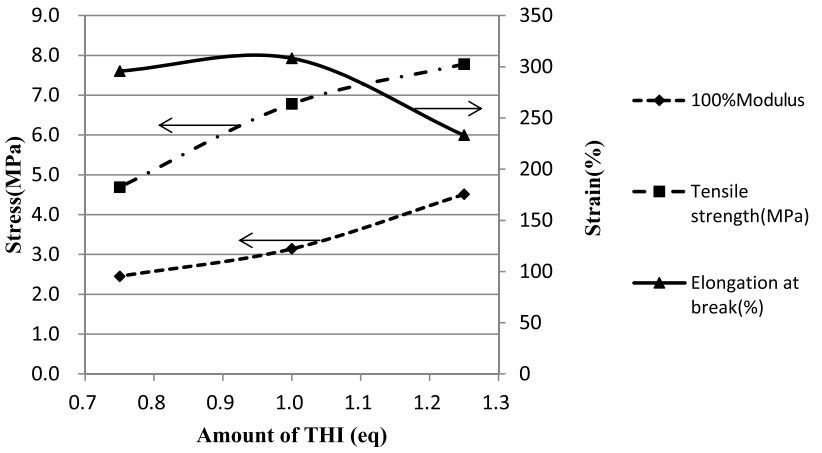

Figure 3. Correlation between amount of THI and stress or strain in the presence of 2.5 phr of organic clay.

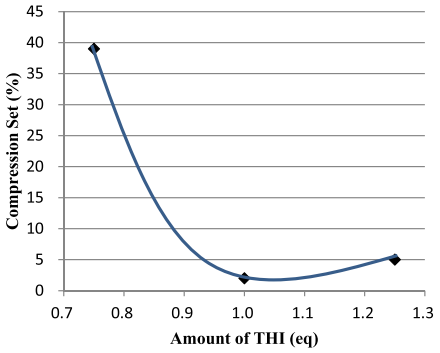

Figure 4. Correlation between amount of THI and the compression set in the presence of 2.5 phr of organic clay.

Table 3. Properties of a Multinetwork Elastomer[a]

glass transition temperature (°C)[b]	−41.2
5% weight loss temperature (°C)[c]	405
recyclability[d]	>10 times
self-healing temperature (°C)[e]	140

[a]Table 2, run 4. [b]Determined by DSC. [c]Determined by TGA. [d]Time of reforming. [e]Self-adhesion ability.

68%). Introduction of a covalent bond can improve the compression set, but deteriorate the self-healing property. This is thought to be due to the difficulty of recombination of the cross-linking. Self-healing materials are important research subjects from the viewpoint of long life and maintenance free, and it is shown that the MNE can be expected to be applied as a self-healing material.[18,19]

2.4. Analysis of Structure. *2.4.1. Transmission Electron Microscope (TEM) Analysis.* Figure 5 shows the TEM image of a multinetwork elastomer (MNE, Table 1 run 3). The added clay can be confirmed to have a black streak shape. The clay size is 200−500 nm and is stacked at intervals of several ten nm. The clay is oriented in the direction of the arrow in Figure 5. Since the sheet was made by press molding, the orientation does not occur normally. However, the clay seems to be oriented. It is considered that the cross-linking is formed by hydrogen bonding between the carboxyl group and the clay surface. The orientation may affect the improvement of tensile properties.

2.4.2. Dynamic Mechanical Analysis (DMA). DMA measurements have also confirmed an increase in tan δ, which indicates hysteresis energy, by adding of organic clay. This

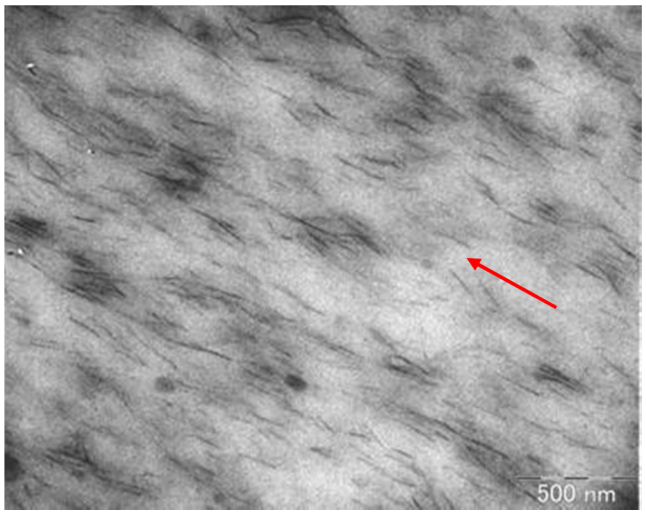

Figure 5. TEM image of a multinetwork elastomer (MNE).

supports that tensile properties are improved by energy dissipation in the multinetwork system (THI and organic clay), compared to the HB + CB system (THI) (Figure 6).

2.4.3. Atomic Force Microscopy (AFM) Measurement. AFM measurement of the rubber surface was performed in viscoelastic mode to sense the Young's modulus of the sample (Figure 7). The yellow part of the image corresponds to the high elasticity and the purple part corresponds to the low elasticity.

In the PB system (organic clay), the low-elasticity part (purple) forms a domain of about 20 to 30 nm, and the high-elastic part (yellow) surrounds the area. The low-elastic purple part can be widely observed, and the high-modulus portion is thin like a thread.

In the HB + CB system (THI), the high-elastic yellow part spreads throughout the sample, but the domain size of the low-modulus portion is the same as about 20−30 nm. On the other hand, in the multinetwork system (THI and organic clay, HB + CB + PB), the domain size of the low modulus was slightly reduced, an intermediate modulus of elasticity was widely observed overall, and the size of the low-modulus part is uneven. That is, the modulus of elasticity is dispersed.

2.4.4. Small-Angle Neutron Scattering (SANS) Analysis. The overall scattering intensity is high over the entire wave number in the case of HB + CB system (THI) and scattering peaks are observed near $q = 0.03$ Å^{-1} of wave number. This is $d =$

https://doi.org/10.1021/acsomega.1c04633
ACS Omega 2021, 6, 31168−31176

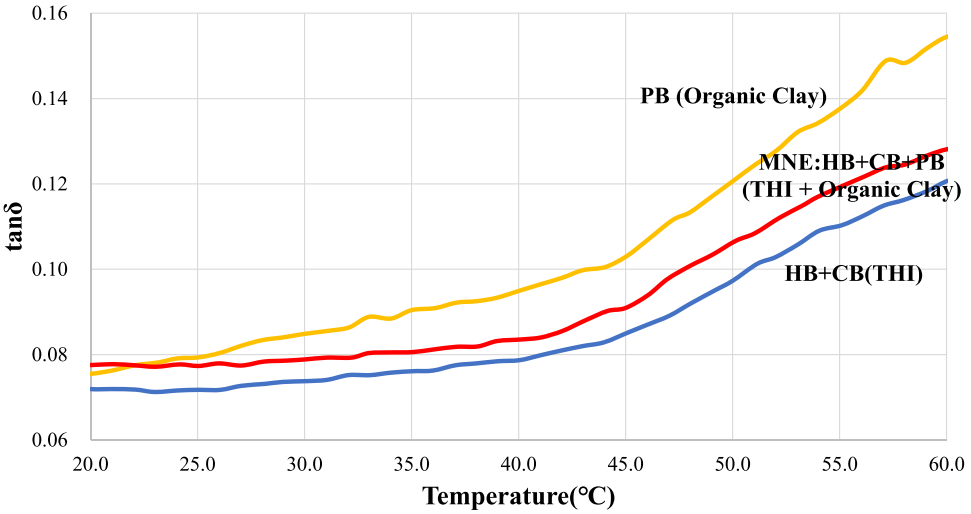

Figure 6. DMA graph of the obtained elastomer synthesized with 1 equiv of THI and/or 1 phr of organic clay. MNE: multinetwork elastomer, HB: hydrogen bond, CB: covalent bond, PB: clay plane bond.

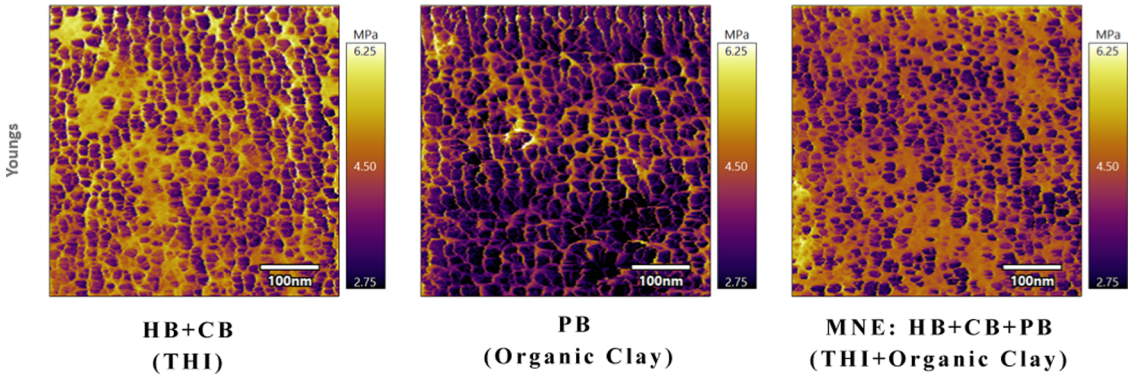

Figure 7. AFM images of the elastomers synthesized from 1 equiv of THI and/or 1 phr of organic clay. MNE: multinetwork elastomer, HB: hydrogen bond, CB: covalent bond, PB: clay plane bond.

20.9 nm (=$2\pi/0.03$) when converted to real space size. This size matches the domain size (about 20−30 nm) of the low-modulus portion as confirmed in the previous AFM image. It may represent the spacing of the high-modulus portion by the cross-linking portion. In the case of the PB system (organic clay), the peak of scattering is observed near q = 0.03 Å^{-1} and the scattering intensity is greatly reduced in the region with a large wave number compared to the sample of THI. The peak of 0.03 Å^{-1} may indicate the aggregate structure of the acid anhydride structure. Since the peak is the same as the peak in the HB + CB system, the size of the collective structure may not change even if cross-linked. Since the size of clay observed in TEM is 200−500 nm, it is thought that the clay cannot be observed in this range of Figure 8.

On the other hand, in the multinetwork system (THI and organic clay, HB + CB + PB), the scattering intensity near the peak is greatly reduced, and concentration fluctuations of 5 to 50 nm size are reduced. This result is consistent with the results of AFM, and the dispersion state of cross-linking points seems to be more uniform (Figure 8).

2.4.5. Infrared Spectroscopy (IR) Measurement. By adding organic clay to hydrogen bonds + covalent bonds (HB + CB), it was confirmed that a new absorption peak appeared in 1716 cm^{-1} in addition to the absorption of carboxyl groups of 1701 and 1734 cm^{-1} as shown in Figure 9. This absorption is thought

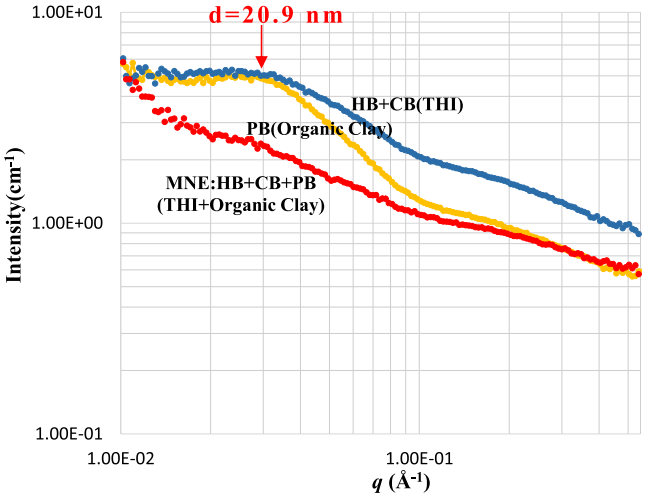

Figure 8. SANS profiles of the elastomers synthesized from 1 equiv of THI and/or 1 phr of organic clay. MNE: multinetwork elastomer, HB: hydrogen bond, CB: covalent bond, PB: clay plane bond.

to be derived from the hydrogen bonding of the carboxyl groups and clay.

2.5. Speculation of the Network Structure. The speculated network structure of the cross-linking point is

https://doi.org/10.1021/acsomega.1c04633
ACS Omega 2021, 6, 31168−31176

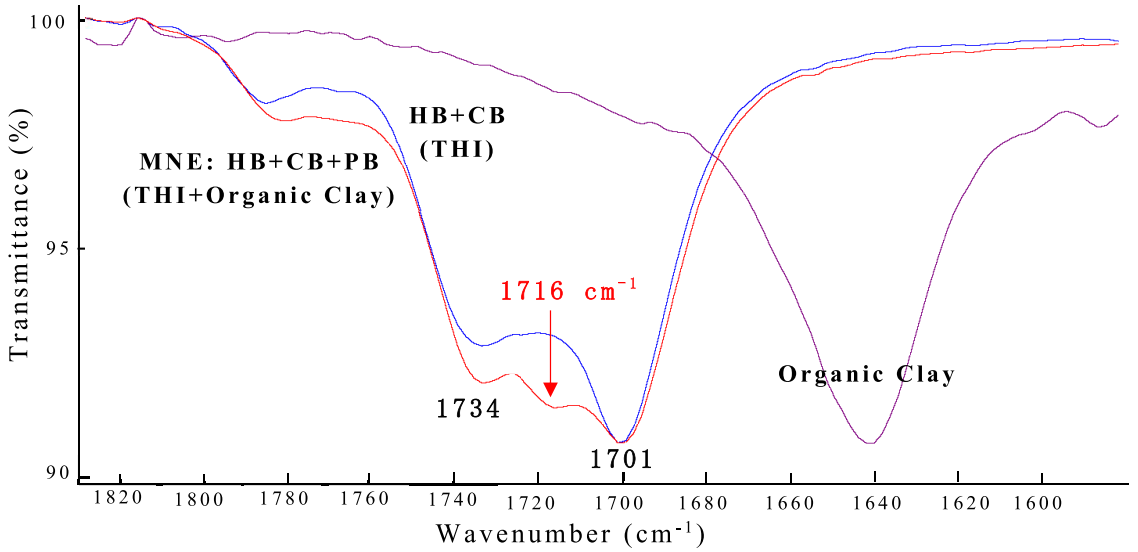

Figure 9. IR spectra of the obtained elastomer synthesized with 1 equiv of THI, and 1 equiv of THI with 1 phr of organic clay. MNE: multinetwork elastomer, HB: hydrogen bond, CB: covalent bond, PB: clay plane bond.

shown in Figure 10. When the covalent bonds of ester were generated by the reaction of the maleic anhydride moiety and the hydroxyl group of THI, the carboxylic acids were generated at the same time. The isocyanurate ring can make complicated hydrogen bonds with the carboxylic acid and the ester. Moreover, the organic clay can also make hydrogen bonds with carboxylic acids and the isocyanurate rings.

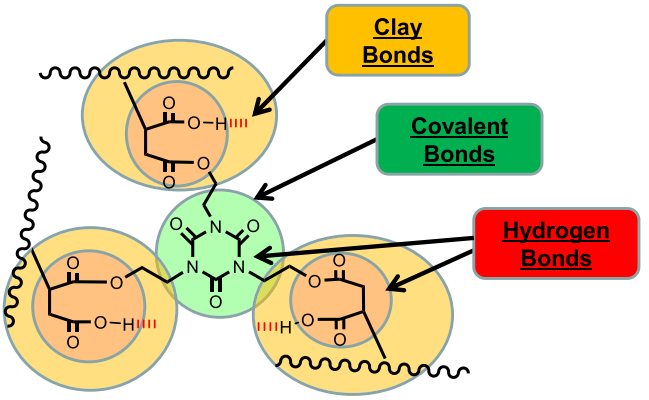

Figure 10. Structure of the cross-linking point.

Since the TEM image shows good dispersion and orientation of the organic clay, the structure of the elastomer is speculated to be as shown in Figures 11 and 12. The polymer chains are cross-linked by hydrogen bonds and covalent bonds. Moreover, the carboxylic acids and isocyanurate rings of polymer may make hydrogen bonds with the clay surface and de-localize the overall cross-linking points.

The covalent bond cross-link contributed to improve the compression set by preventing the polymer chain flow. The hydrogen bond cross-link contributes to improving the flowability because of the cleavage under heating. The clay plane bond seems to nonlocalize the overall cross-linking points and increase the hysteresis energy to improve the tensile properties.

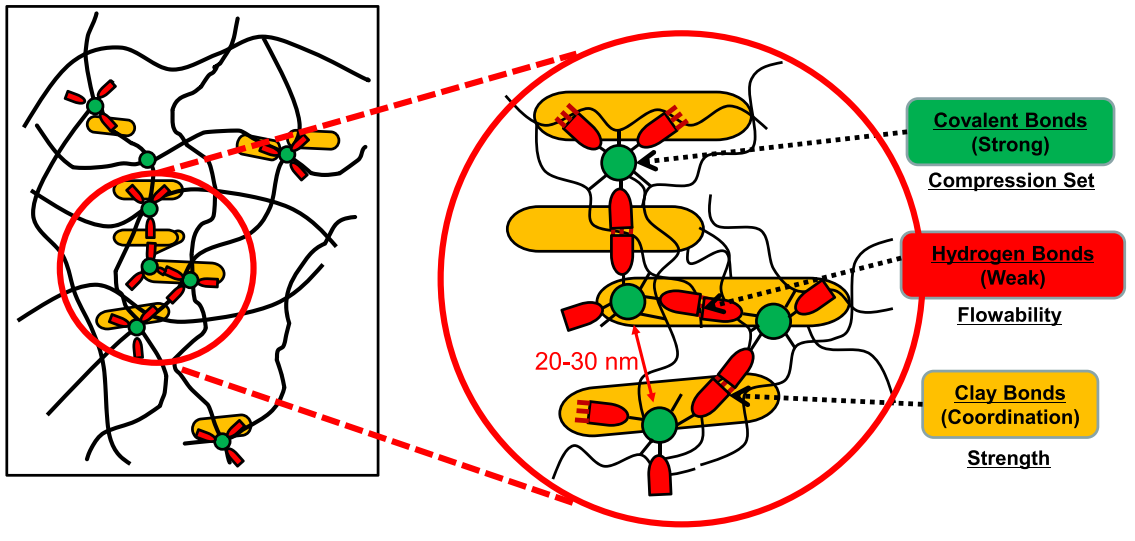

Figure 11. Schematic structure of the multinetwork elastomer.

https://doi.org/10.1021/acsomega.1c04633
ACS Omega 2021, 6, 31168−31176

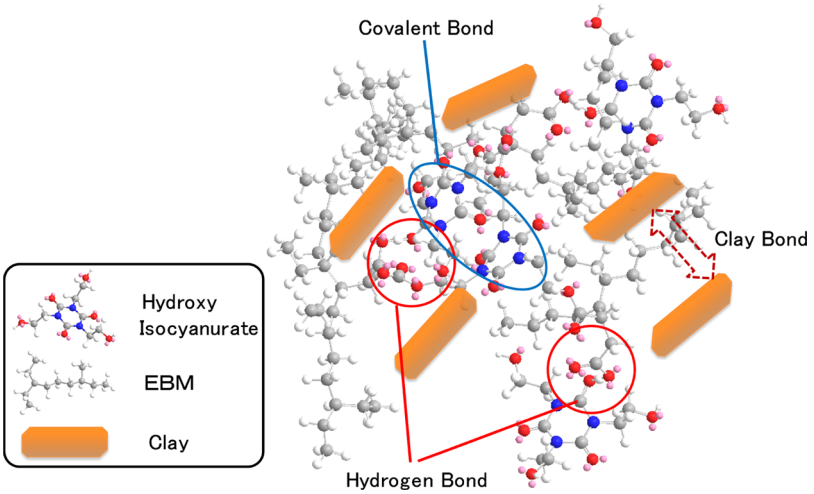

Figure 12. Schematic structure of the multinetwork elastomer.

3. CONCLUSIONS

A high-performance elastomer was obtained by a multinetworking system of a covalent bond, hydrogen bond, and clay plane bond. By using each feature of the cross-linking bonds, the thermoplastic elastomer shows excellent compression set resistance, good flowability, and high tensile properties. The hydrogen bond shows flowability due to the bond cleavage under heating. The covalent bond contributes to the low compression set by preventing the polymer chain flow. Moreover, the clay plane bond affects the tensile properties by de-localization of the entire cross-link and increase of hysteresis energy between the clay plane surface and hydrogen bond cross-link. Furthermore, the self-healing properties and high heat resistance and recyclability were also observed.

4. EXPERIMENTAL SECTION

4.1. Materials. •3-Amino-1,2,4-triazole (ATA): Kanto Chemical Co., Inc.

•Tris(2-hydroxyethyl)isocyanurate(THI): Nissei Co., NISSEI THEIC.

•Organic clay: Kunimine Industries Co., Ltd., Kunifil D-36, Montmorillonite treated with Dimethyldioctadecylammonium chloride.

•Polyether polyol: ADEKA Corporation, EDP-1100, Ethylenediamine, propylene oxide type, tetra functional type, OH: 3.92 mmol g^{-1}.

•Sulfamide: Kanto Chemical Co., Inc.

•Antioxidant: BASF Schweiz AG, Irganox1010, Pentaerythritol tetrakis(3-(3,5-di-tert-butyl-4-hydroxyphenyl)-propionate) (PBP).

•Maleated ethylene-butene elastomer: MITSUI CHEMICALS, INC, Tafmer MH5020, MFR: 1.2 g/10 min (230 °C), density: 866 kg m^{-3}, Hardness(Shore A)55, ethylene content: 56 wt %, maleated ratio: 1.47 wt %.

IR (ATR-FTIR): 2959, 2918, 2850 (C−H stretching), 1790 (C═O (from maleic anhydride)), 1461 ($-CH_2-$ vending), 1378 ($-CH_3$ vending), 1263, 1021, 771, 719 cm^{-1}.

Solid-state ^{13}C NMR (499.7 MHz) δ in ppm: 10.87 ($-\underline{C}H_3$), 25.96 (branch $-\underline{C}H_2-$), 26.84, 29.92, 33.29 ($-\underline{C}H_2-CH(-\underline{C}H_2-)-\underline{C}H_2-$), 38.85 ($-CH_2-\underline{C}H(-CH_2-)-CH_2-$).

Elemental analysis. Found: C, 83.9; H, 14.2; N, <0.1; O, 0.8.

Dynamic viscoelasticity analysis. T_g: −40.4 °C.

TGA analysis (heating rate; 10 °C min^{-1}, under N_2) T_{d5}: 435.4 °C.

•Synthesis of hydrogen bond elastomer: addition reaction of ATA to maleated ethylene-butene elastomer (Table 1 run 1).

A mixture of 100 g (0.015 mol; maleic anhydride unit) of maleated ethylene-butene elastomer and 0.1 g (1.0 phr: parts per hundred rubber) of PBP was masticated in 20 rpm at 180 °C for 2 min in an internal mixer. Subsequently, 1.26 g (0.015 mol) of ATA was added and kneaded in 20 rpm at 180 °C for 12 min in an internal mixer. The addition of ATA to the maleated ethylene-butene elastomer was identified by IR analysis, which showed the disappearance of peaks based on acidic anhydride and the existence of peaks due to imide.

IR (ATR-FTIR): 2959, 2918, 2850 (C−H stretching), 1726 (C═O), 1461 ($-CH_2-$ vending), 1379 ($-CH_3$ vending), 1264, 771, 720 cm^{-1}.

Solid-state ^{13}C NMR (499.7 MHz) δ in ppm: 10.87 ($-\underline{C}H_3$), 25.96 (branch $-\underline{C}H_2-$), 26.84, 29.92, 31.89, 32.55, 33.36 ($-\underline{C}H_2-CH(-\underline{C}H_2-)-\underline{C}H_2-$), 38.85 ($-CH_2-\underline{C}H-(-CH_2-)-CH_2-$).

Dynamic viscoelasticity analysis. T_g: −53.2 °C.

TGA analysis (heating rate; 10 °C min^{-1}, under N_2) T_{d5}: 435.3 °C.

•Synthesis of hydrogen bond, and covalent bond elastomer: addition reaction of THI to maleated ethylene-butene elastomer (Table 1 run 2).

A mixture of 100 g (0.015 mol; maleic anhydride unit) of maleated ethylene-butene elastomer and 0.1 g (1.0 phr) of PBP was masticated in 20 rpm at 180 °C for 2 min in an internal mixer. Subsequently, 1.31 g (0.005 mol, OH: 0.015 mol) of THI was added and kneaded in 20 rpm at 180 °C for 8 min in an internal mixer. The addition of THI to the maleated ethylene-butene elastomer was identified by IR analysis, which showed the disappearance of peaks based on acid anhydride and the existence of peaks due to ester.

IR (ATR-FTIR): 2959, 2919, 2850 (C−H stretching), 1734 (C═O), 1701 (C═O), 1461 ($-CH_2-$ vending), 1379 ($-CH_3$ vending), 1265, 1170, 1097, 969, 771, 720 cm^{-1}.

Solid-state ^{13}C NMR (499.7 MHz) δ in ppm: 10.87 ($-\underline{C}H_3$), 23.84, 26.03 (branch $-\underline{C}H_2-$), 26.84, 29.92, 31.89, 32.29 ($-\underline{C}H_2-CH(-\underline{C}H_2-)-\underline{C}H_2-$), 38.85 ($-CH_2-\underline{C}H-(-CH_2-)-CH_2-$).

Elemental analysis. Found: C, 84.3; H, 14.2; N, <0.1; O, 1.4.

https://doi.org/10.1021/acsomega.1c04633
ACS Omega 2021, 6, 31168−31176

Dynamic viscoelasticity analysis. T_g: −53.0 °C.

TGA analysis (heating rate; 10 °C min^{-1}, under N_2) T_{d5}: 428.0 °C.

•Synthesis of hydrogen bond, covalent bond, and clay plane bond elastomer: addition reaction of THI and organic clay to maleated ethylene-butene elastomer (Table 1 run 3).

A mixture of 100 g (0.015 mol; maleic anhydride unit) of maleated ethylene-butene elastomer and 0.1 g (1.0 phr) of PBP was masticated in 20 rpm at 180 °C for 2 min in an internal mixer. Subsequently, 5 g of organic clay was added and kneaded in 20 rpm at 180 °C for 4 min. Finally, 1.31 g (0.005 mol, OH: 0.015 mol) of THI was added and further kneaded in 20 rpm at 180 °C for 8 min. The addition of THI to the maleated ethylene-butene elastomer was identified by IR analysis, which showed the disappearance of peaks based on acid anhydride and the existence of peaks due to ester.

IR (ATR-FTIR): 2959, 2919, 2850 (C−H stretching), 1734 (C═O), 1716 (C═O), 1701 (C═O), 1693, 1461 (−CH_2− vending), 1379 (−CH_3 vending), 1264, 1094, 1037, 969, 767, 720 cm^{-1}.

Elemental analysis. Found: C, 84.1; H, 14.5; N, <0.1; O, 1.3.

Dynamic viscoelasticity analysis. T_g: −51.9 °C.

TGA analysis (heating rate; 10 °C min^{-1}, under N_2) T_{d5}: 420.0 °C.

•Synthesis of elastomer having hydrogen bond, covalent bond, and clay plane bond: addition reaction of sulfamide and clay to maleated ethylene-butene elastomer (Table 1 run 4).

IR (ATR-FTIR): 2959, 2919, 2850 (C−H stretching), 1714 (C═O), 1462 (−CH_2− vending), 1379 (−CH_3 vending), 1299, 1263, 1092, 1036, 916, 772, 720 cm^{-1}.

Solid-state ^{13}C NMR (499.7 MHz) δ in ppm: 10.80 (−CH_3), 25.96 (branch −$\underline{C}H_2$−), 26.77, 29.84, 32.48, 33.29 (−$\underline{C}H_2$−CH(−$\underline{C}H_2$−)-$\underline{C}H_2$−), 38.78 (−CH_2−$\underline{C}$H(−CH_2−)−CH_2−).

•Synthesis of hydrogen bond, covalent bond, and clay plane bond elastomer: addition reaction of polyetherpolyol and clay to maleated ethylene-butene elastomer (Table 1 run 5).

IR (ATR-FTIR): 2959, 2919, 2850 (C−H stretching), 1724 (C═O), 1461 (−CH_2− vending), 1378 (−CH_3 vending), 1299, 1264, 1096, 1037, 772, 720 cm^{-1}.

Solid-state ^{13}C NMR (499.7 MHz) δ in ppm: 10.80 (−CH_3), 25.96 (branch −$\underline{C}H_2$−), 26.77, 29.84, 31.82, 33.29 (−$\underline{C}H_2$−CH(−$\underline{C}H_2$−)−$\underline{C}H_2$−), 38.78 (−CH_2−$\underline{C}$H(−CH_2−)−CH_2−).

4.2. Procedure of Making Sheets. Sheets of the obtained elastomers were prepared by press molding at 200 °C for 8 min under 16 MPa of pressure and successive cold press molding for 2 min under the same pressure. Sheets of size 2 mm × 15 cm × 15 cm were obtained.

4.3. Hardness. Shore A hardness is measured by stacking 5 pieces of the obtained sheets according to ASTM D 2240.

4.4. Tensile Properties. Stress−strain properties were measured at a speed of 500 mm min^{-1} on a Toyo Seiki Seisaku-sho Strograph VE according to JIS K6251 using type 3 dumbbells. 100% modulus (M_{100}) [MPa], 300% modulus (M_{300}) [MPa], tensile strength (T_B) [MPa], and elongation at break (E_B) [%] were measured at room temperature.

4.5. Compression Set. The compression set was measured according to JIS K6262. A disk-shaped sample was cut from the sheet, and the height was adjusted to 12.5 ± 0.5 mm by stacking 7 or 8 pieces of the disk-shaped sample. The stacked columnar sample was compressed 25% from the original height and kept at 70 °C for 22 h. After releasing the pressure, the sample was kept at room temperature for 30 min and the height was measured. By comparing the heights before and after the experiment, the compression set ratio was calculated.

4.6. Dynamic Mechanical Analysis (DMA). Glass transition temperature (T_g) and hysteresis energy were measured by a dynamic viscoelasticity analyzer using a Rheogel-E4000 (UBM Co., Ltd. Tension mode) at 3 °C min^{-1} heating rate, 0.1% strain, and 10 Hz frequency. The T_g values for each elastomer were determined from the peak value of tan δ. The hysteresis energy was estimated from the tan δ value.

4.7. 5% Weight Decrease Temperature. The 5% weight decrease temperature (T_{d5}) was measured by a thermogravimetric analyzer on a TA instrument model DSC2920 at 10 °C min^{-1} heating rate under N_2.

4.8. Self-Healing Property. The sheet (1 mm × 5 cm × 5 cm), which was cut in 5 mm length, was heated by elevating the temperature at 20 °C from 60 °C for 10 min. The self-healing temperature was determined by adhering of the cutting part.

4.9. Infrared Analyses (IR). Infrared (IR) analyses were performed using a Thermo Fisher Scientific Corporation model Nicolet iS 10.

4.10. Solid-state ^{13}C NMR Analyses. Solid NMR analyses were performed using a Varian model NMR Oxford AS500.

4.11. Recyclability. Recyclability was evaluated by the capability of reforming more than 10 times.

4.12. AFM Measurement. The AFM measurement in this study was performed using a commercial AFM system OXFORD INSTRUMENTS Asylum Research Jupiter XR with a Fast Force Map mode (Setpoint 100 nN, Points: 256, ForceDist: 1.50 μm, Z rate: 200 Hz). The cantilever used in this mode was made of Asylum Research (AC240TS-R3) with a nominal spring constant of 2 N m^{-1} and a tip radius of 7 nm. Before the measurement, an actual spring constant of the cantilever was measured by Sader's method.

4.13. Small-Angle Neutron Scattering (SANS) Measurement. Neutron small-angle scattering measurements were performed at BL-20 at the Ibaraki Prefectural Material Structure Analyzer (iMATERIA) in the Materials and Life Science Experimental Faculty (MLF), Japan Proton Accelerator Research Complex (J-PARC), Tokai Village, Ibaraki Prefecture, Japan, under a user program (Proposal No. 2020BM0001).

The measurement samples (1 mm × 15 mm Φ) were swollen with 150 wt % of toluene-d_8 to visualize the cross-linking structure. The two-dimensional scattering was obtained regarding detector sensitivity, and a one-dimensional scattering profile was obtained by taking the background in consideration of the transmittance and taking the circular average. It was converted to absolute strength using a grassy carbon standard sample.

AUTHOR INFORMATION

Corresponding Author

Keisuke Chino − *Resin Treatment & Engineering Group, HPM Research & Development Dept., High Performance Materials Company, ENEOS Corporation, Yokohama, Kanagawa 231-0815, Japan;* orcid.org/0000-0003-0205-9404; Phone: +81-45-415-7692; Email: chino.keisuke@eneos.com

Complete contact information is available at: https://pubs.acs.org/10.1021/acsomega.1c04633

https://doi.org/10.1021/acsomega.1c04633
ACS Omega 2021, 6, 31168−31176

Notes

The author declares no competing financial interest.

■ ACKNOWLEDGMENTS

The author would like to thank Professor Satoshi Koizumi, Dr. Tomoki Maeda, Dr. Takumi Inada of Ibaraki University, and Dr. Yukio Morii of Radiation Application Development Association (RADA) for SANS analysis, and also Nobuharu Kimura, Yoshimu Iwanami, Rusaka Sato, and Shota Fujii of ENEOS corporation for supporting the chemical analyses and experiments.

■ REFERENCES

(1) Singh, N. K.; Lesser, A. J. Mechanical and thermo-mechanical studies of double networks based on thermoplastic elastomers. *J. Polym. Sci., Part B: Polym. Phys.* **2010**, *48*, 778−789.
(2) Roland, C. M.; Warzel, M. L. Orientation effects in rubber double networks. *Rubber Chem. Technol.* **1990**, *63*, 285−297.
(3) Santangelo, P. G.; Roland, C. M. The mechanical behavior of double network elastomers. *Rubber Chem. Technol.* **1994**, *67*, 359−65.
(4) Andrews, R. D.; Tobolsky, A. V.; Hanson, E. E. The theory of permanent set at elevated temperatures in natural and synthetic rubber vulcanizates. *J. Appl. Phys.* **1946**, *17*, 352−361.
(5) Manik, S. P.; Banerjee, S. Studies on dicumylperoxide vulcanization of natural rubber in presence of sulfur and accelerators. *Rubber Chem. Technol.* **1969**, *42*, 744−758.
(6) Manik, S. P.; Banerjee, S. Effect of sulfur and dicumyl peroxide on vulcanization of natural rubber with tetramethylthiuram disulfide and zinc oxide. *Rubber Chem. Technol.* **1970**, *43*, 1294−1310.
(7) Gong, J. P. Materials both tough and soft. *Science* **2014**, *344*, 161−162.
(8) Haraguchi, K. Synthesis and properties of soft nanocomposite materials with novel organic/inorganic network structures. *Polym. J.* **2011**, *43*, 223−241.
(9) Chino, K.; Ashiura, M. Themoreversible cross-linking rubber using supramolecular hydrogen-bonding networks. *Macromolecules* **2001**, *34*, 9201−9204.
(10) Chino, K.; Ashiura, M.; Natori, J.; Ikawa, M.; Kawazura, T. Thermoreversible crosslinking rubber using supramolecular hydrogen bonding networks. *Rubber Chem. Technol.* **2002**, *75*, 713−723.
(11) Chino, K.; Ashiura, M.; Natori, J.; Kawazura, T. Development of thermoreversible crosslinking rubber using supramolecular hydrogen bonding networks. *Nippon Gomu Kyokaishi* **2002**, *75*, 482−487.
(12) Chino, K. Thermo reversible crosslinking rubber using supramolecular hydrogen bonding networks. *KGK, Kautsch. Gummi Kunstst.* **2006**, *59*, 158−162.
(13) Andrews, E. H. High strain rate testing of plastics. 1. Shock tube technique. *J. Mater. Sci.* **1974**, *9*, 887−894.
(14) Cunneen, J. I.; Portet, M. Rubber derivatives. *Encycl. Polym. Sci. Technol.* **1970**, *12*, 304−327.
(15) Ceresa, R. J. The chemical modification of polymers. *Sci. Technol. Rubber* **1978**, 455−488.
(16) Akagi, Y.; Gong, J. P.; Chung, U.; Sakai, T. Transition between phantom and affine network model observed in polymer gels with controlled network structure. *Macromolecules* **2013**, *46*, 1035−1040.
(17) Kabashima, S.; Tanaka, S.; Kageyama, M.; Yoshikawa, I.; Araki, K. Hydrogen-bond-directed 2-D sheet assemblies of sulfamide derivatives: formation of giant vesicles with patchwork-like surface pattern. *Langmuir* **2011**, *27*, 8950−8955.
(18) Wei, H.; Yang, Y.; Huang, X.; Zhu, Y.; Wang, H.; Huang, G.; Wu, J. Transparent, robust, water-resistant and high barrier self-healing elastomers reinforced with dynamic supramolecular nanosheets with switchable interfacial connections. *J. Mater. Chem. A* **2020**, *8*, 9013−9020.
(19) Chen, Y.; Guan, Z. Self-assembly of core−shell nanoparticles for self-healing materials. *Polym. Chem.* **2013**, *4*, 4885−4889.

https://doi.org/10.1021/acsomega.1c04633
ACS Omega 2021, 6, 31168−31176